Analytical Methods

DOI: 10.1002/anie.201207348

Metabolic Differences in Microbial Cell Populations Revealed by Nanophotonic Ionization**

*Bennett N. Walker, Cory Antonakos, Scott T. Retterer, and Akos Vertes**

Growing interest in functional genomics[1] has resulted in technological breakthroughs in advanced proteomics, including the intracellular microproteomic analysis of tissues and cells.[2] Quantitative differences in the proteome at the single-cell level can be detected by flow cytometry and fluorescence,[3] as well as mass spectrometry,[4,5] whereas microbial single cell metabolomics has not progressed as rapidly because it involves studying compounds of larger chemical variety, higher turnover rates, and lower molecular weights, coincident with the mass range of common contaminants. Owing to the low copy number of some intracellular proteins and the presence of extracellular noise, isogenic cells can exhibit large differences in their metabolic makeup.[6] This metabolic noise, part of cellular differences, is poorly characterized because it requires the multicomponent analysis of severely volume-limited samples, that is, individual microbial cells. A technique that can capture metabolic variations for a large fraction of the hundreds to thousands of metabolites in single cells or small populations requires a combination of ultra-low limits of detection, high selectivity, and high quantitation capability.[7–9]

Currently, most metabolic studies are conducted using fluorescence measurements,[10] NMR spectroscopy,[11,12] or mass spectrometry (MS).[8,13–18] Fluorescence measurements provide an ultra-low limit of detection and high selectivity[10] but typically require labeling of selected metabolites, making the process laborious, time consuming, and potentially invasive. NMR and MS are often considered to be complementary techniques; NMR is viewed as a universal detector that does not rely on separation but lacks the sensitivity to analyze single cells. Mass spectrometry is a highly sensitive technique, but to achieve sufficient selectivity and peak capacity, it is often coupled with separation techniques. LC–MS[19] and GC–MS[20–23] are efficient methods to detect and quantitate thousands of metabolites in complex extracts from large cell populations. These methods require thousands to millions of cells to achieve a high coverage of the metabolome. The analysis of cellular metabolites using secondary ion MS (SIMS),[24,25] MALDI MS,[16,26] and laser desorption ionization (LDI) on nanoporous structures[8] shows promise for large-scale metabolomic studies.

Recently, we introduced silicon nanopost arrays (NAPA) as a matrix-free LDI-MS method with highly enhanced ion yields and photonic properties.[27–29] A typical NAPA chip is comprised of over two million ordered monolithic silicon nanoposts (see inset in Figure 1 b). The array is defined by the height, H, diameter, D, and periodicity, P, of the posts. Posts of a given diameter exhibit an ion yield resonance at a particular aspect ratio (Supporting Information, Figure S1).

In this study, *Saccharomyces cerevisiae* was chosen for exploring the metabolome in small cell populations and single cells, because the yeast metabolome and metabolic networks are relatively small and have been extensively analyzed.[30] Without distinguishing chemical species in the different cellular compartments, there are 584 known metabolites that take part in 1175 reactions organized into 94 major biochemical pathways.[31] We demonstrate that LDI from NAPA can capture metabolic changes in single yeast cells and small cell populations owing to oxidative stress. Intra- and inter-population differences can also be examined by this method.

AFM imaging of a yeast cell on a NAPA before and after laser exposure showed that, as a consequence of the laser radiation, the intracellular contents were released onto the nanostructure (Figure 1 a). Our results indicate that the limit of detection for the LDI of various organic and biomolecules from NAPA can reach approximately 800 zeptomoles (measured for verapamil standards).[33] Because the estimated amounts of some primary metabolites, for example, amino acids, in an approximately 30 fL yeast cell are in the 10 amol to 30 fmol range, the sensitivity of the NAPA technique should be sufficient for single microbial-cell analysis.

Small populations ($1 \le n \le 80$) of *S. cerevisiae* were directly deposited and analyzed on NAPA. In the mass range of small metabolites (50–500 Da), the mass spectra generated by LDI resulted in numerous peaks yielding up to 108 assignments (Figure 1 b) that corresponded to 18 % of the known metabolome. Table S1 (Supporting Information) shows the list of metabolite assignments derived from LDI-MS using NAPA. These tentative assignments were curated from multiple datasets, assuming protonation and addition of Na^+ or K^+ ions in the positive ion mode, as well as proton loss

[*] Dr. B. N. Walker, C. Antonakos, Prof. A. Vertes
Department of Chemistry, The George Washington University
Washington, DC 20052 (USA)
E-mail: vertes@gwu.edu
Homepage: http://www.gwu.edu/~vertes
Dr. S. T. Retterer
Oak Ridge National Laboratory
Oak Ridge, TN 37831 (USA)

[**] Support from the Division of Chemical Sciences, Geosciences, and Biosciences, Office of Basic Energy Sciences of the U.S. Department of Energy (Grant DE-FG02-01ER15129) is gratefully acknowledged. A portion of this research (nanofabrication) was conducted at the Center for Nanophase Materials Sciences, which is sponsored at Oak Ridge National Laboratory by the Scientific User Facilities Division, Office of Basic Energy Sciences, U.S. Department of Energy.

Supporting information for this article is available on the WWW under http://dx.doi.org/10.1002/anie.201207348.

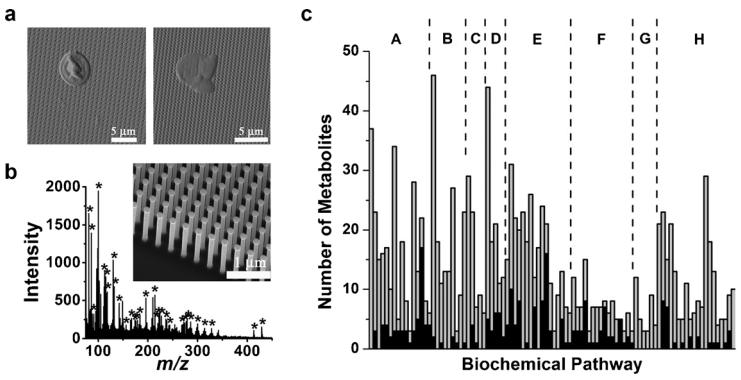

Figure 1. a) AFM images of a single *S. cerevisiae* cell on NAPA before (left) and after (right) laser exposure. As the cell wall is ruptured by the laser pulse, the intracellular metabolites are exposed and ionization occurs. b) Laser irradiation of 78 yeast cells on the NAPA (* = identified metabolite). Inset: SEM image of the NAPA used herein. c) Bar graph comparing the number of metabolites involved in particular biochemical pathways (gray) to the number of identified metabolites (black). The major biochemical pathways are as follows: A) amino acid biosynthesis, B) fatty acid and lipid biosynthesis, C) carbohydrate biosynthesis, D) nucleoside/tide biosynthesis, E) biosynthesis of cofactors, prosthetic groups, and electron carriers, F) amino acid degradation, G) carbohydrate and sugar degradation, and H) all other biochemical pathways, including the TCA cycle.

for the formation of negative ions. The assignments were based on mass accuracy with a $\Delta m/z \leq 0.06$ cutoff from metabolite searches in the *Saccharomyces* Genome Database (SGD) (http://www.yeastgenome.org/). Further validation of most of the assignments requires tandem MS and functional studies.

Based on these LDI-MS measurements, Figure 1c shows the coverage of individual metabolic pathways grouped into families. Table S2 summarizes the aggregated metabolite coverage for families of biochemical pathways and super-pathways. The metabolite coverage was calculated as a percentage of the total number of metabolites in the pathway family. Two additional examples of high-metabolite coverage are shown in Figure S2 for the super-pathway for threonine and methionine biosynthesis, and the super-pathway for the tricarboxylic acid (TCA) cycle and the glyoxylate cycle. Counting the pathways that had at least one metabolite assigned in the spectra, 67% coverage of the 94 major pathways was established (see Figure S2 for the coverage of two selected biochemical pathways).

As metabolite turnover rates in microorganisms are faster than changes observed in the genome and the proteome, intracellular metabolic content can be sensitive to analysis conditions. In addition, significant metabolic differences can be expected within and among cell populations.[32] Therefore, analyzing the variances between the spectra of individual cells, rather than the large populations required for LC–MS[19] and GC–MS,[20] can reveal intra- and inter-population differences.

Separation and analysis techniques for single animal cells have recently been introduced and are currently used in various research laboratories.[9,10] These metabolic studies involve either the analysis of only a few chemical species using fluorescence, or require the use of larger cells with volumes of 500 fL or greater. NAPA has the sensitivity and quantitation capabilities (Figure S3) to enable the analysis of single yeast cells with approximately 30 fL volume for multiple metabolites.[33] Figure 2a shows the LDI mass spectrum of a single yeast cell deposited onto the NAPA surface with minimal interference from background ions. The identified peaks correspond to up to 24 species or up to 4% of the known metabolome with at least one metabolite detected from 29% of the major biochemical pathways. The pathways with the highest coverage were the biosynthesis of amino acids, nucleotides, and cofactors. Minimal background interference and multispecies coverage represent promising attributes for this label-free single-cell analysis method.

Ion abundance changes in NAPA spectra enable the quantitative metabolic analysis of small cell populations and single cells. Comparing the spectra for cell population sizes of $n = 1$ and 79 in Figure 2a,b, respectively, indicates more abundant peaks from a larger number of species in the multicell spectrum. By plotting ion intensities for four common amino acids (proline, lysine, methionine, and cysteine) as a function of absolute amounts

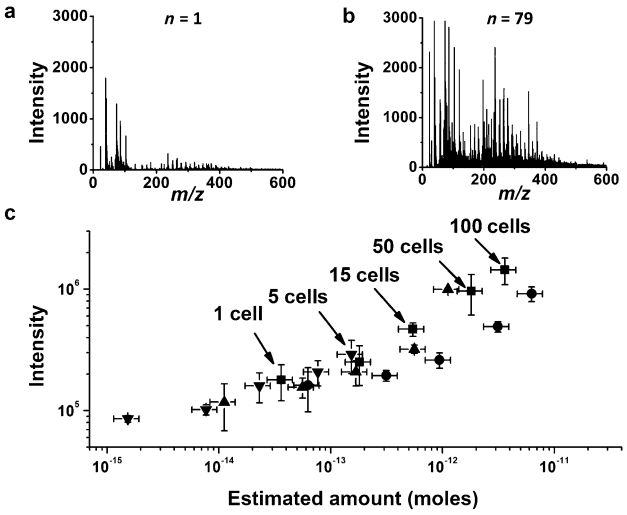

Figure 2. a) Mass spectrum of a single *S. cerevisiae* cell by LDI-MS from NAPA. b) Mass spectrum from 79 yeast cells by LDI-MS from NAPA. c) Ion intensities for four amino acids (proline (■), lysine (●), methionine (▲), and cysteine (▼)) as a function of their estimated amounts in small cell populations of increasing size in the $1 \leq n \leq 100$ range. Cell numbers are indicated for proline. The calculated volume of a cell is approximately 30 fL.

estimated for population sizes between $n = 1$ and $n = 100$ from the average biomass composition of *S. cerevisiae*,[31] a quantitative response can be established and analyzed with a dynamic range of up to three orders of magnitude.

Metabolic network reconstruction of *S. cerevisiae* based on genomic information[34] and flux balance analysis can be used to determine the essential reactions, the participating biochemical species, and predict complex intracellular changes that are due to environmental stimuli.[31] Multiple

attempts to establish the metabolic network for *S. cerevisiae* have led to the emergence of consensus models.[35] As the metabolic map is both complex and can undergo functional changes, rapid multispecies verification of the models is necessary. The direct analysis of numerous intracellular yeast metabolites in conjunction with quantitation capabilities, demonstrated in Figure 2c, can be used to verify these models and perhaps resolve ambiguities.

To observe the physiological response in small microbial cell populations, we studied the metabolic changes in *S. cerevisiae* under oxidative stress induced by hydrogen peroxide in the growth medium. Small populations ($n < 80$) of stressed and control cells were studied by LDI-MS from NAPA to determine the up- and downregulation of various metabolites. Orthogonal projections to latent structures discriminant analysis (OPLS-DA) of the spectra indicated that the observed differences between the stressed and control populations were statistically significant.

Studying oxidative stress in small yeast cell populations indicated a metabolic response that resulted in significantly changed metabolite levels (Figure 3; Table S3). To identify the metabolites responsible for most of the variance between the spectra from the stressed and control cell populations, S-plots were constructed. For metabolites corresponding to the points with both high correlation and covariance values (the "wings" of the curve), paired-sample t-tests were conducted with a $p < 0.05$ cutoff to assess if the ion intensity changes were statistically significant. In populations of $n \approx 80$ yeast cells exposed to oxidative stress, 21 statistically significant metabolic changes were identified. An additional ten peaks in the mass spectra showed significant changes, but they remained unassigned.

In the stressed populations, the upregulation of glutathione (a major intracellular redox buffer known to curb oxidative damage) was observed ($p < 0.002$), along with two metabolites involved in its biosynthesis, cysteinylglycine and glutamylcysteine. Although the upregulation of urate, an alternative redox buffer, was also observed, *S. cerevisiae* does not have the gene for urate oxidase (UOX), the enzyme necessary for it to curb hydrogen peroxide.[36] Downregulation of compounds related to folate biosynthesis, responsible for promoting cellular growth, such as amino-4-deoxychorismate and dihydroneopterin phosphate, were also observed ($p < 4 \times 10^{-4}$) indicating that the cells redirected resources from growth to fighting stress.

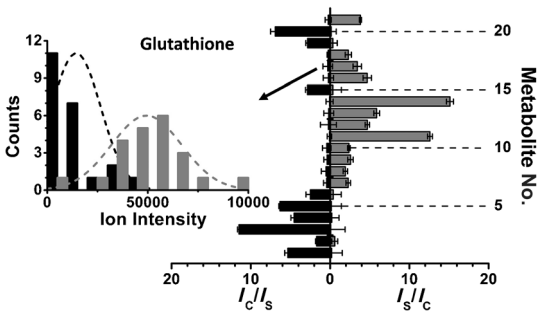

Figure 3. Upregulation of 12 intracellular metabolites (gray bars, right axis) was observed after cells ($n \approx 80$) were exposed to oxidative stress for one hour. Downregulation was seen for another nine intracellular metabolites (black bars, left axis). Inset: histogram of the ion intensity distributions for glutathione with (gray) or without (black) oxidative stress. The shift in the mean of the distribution indicates the inter-population differences.

Comparing the single cell spectra from the two populations (see Figure S4a,b for an example of each) by OPLS-DA indicated clear clustering (Figure S4c) and the absence of strong outliers. The analysis showed that the spectra from the stressed and control groups were well separated even at the single cell level (see the scores plot and the S-plot in Figure S4 and Figure S5a, respectively).

To identify the metabolites responsible for most of the variance between the single cell spectra of the stressed and control populations, an S-plot was generated (Figure S5a). Inspecting the points with high covariance and correlation revealed that threonine and sedoheptulose phosphate were upregulated, whereas dimethylsulfide, proline, and glycerol phosphate were downregulated. These and other compounds with similar parameters in the S-plot can be regarded as putative biomarkers for oxidative stress derived from single-cell studies. The differences in the ion intensity distributions for threonine and dimethylsulfide are apparent from the histograms in Figure S5b,c. Paired-sample t-tests on this data confirmed that these changes were statistically significant with $p < 6 \times 10^{-5}$ for threonine and $p < 4 \times 10^{-5}$ for dimethylsulfide. These examples demonstrate that cellular differences can be captured by single cell analysis using LDI-MS from the NAPA ionization method.

To determine the distributions of the measured ion intensities, spectra from 20 single cells were acquired (Figure S3a). Histograms of the distributions of the relative ion intensities for leucine and serine are shown Figure S3b. Standard deviations of the average ion intensities, derived from the single cell spectra, were used to assess cellular differences. To separate the intra-population differences from the method-related fluctuations, the variance of the latter was determined on standard solution samples representing analyte amounts similar to what was contained in a single cell. The variance of the method was then subtracted from the measured variance to yield the variance owing to cellular differences. Relative standard deviations for the intra-population cellular differences of lysine, methionine, cysteine, and proline were 26%, 30%, 10% and 25%, respectively. Based on the histograms, there were no subpopulations with separate mean averages.

Quantitative investigation of the cellular differences for various metabolites at the single-cell level can aid in the analysis of metabolic noise.[37,38] The histogram in the inset of Figure 3 shows how the ion intensity distribution for glutathione changes as a result of oxidative stress. The shift in the mean of the distribution indicates the inter-population differences. Intra-population differences can be derived from single-cell studies. Figure S5b,c shows the distribution of threonine and dimethylsulfide ion intensities. The widths of the distributions are linked to the intra-population differences, whereas the difference in the means indicate inter-population differences.

Currently, information about microbial physiology is obtained in large cell populations (approximately 106 cells)

through the observation of a single or a few predetermined metabolic markers and/or through labeling.[39] Nanofabrication of NAPA structures enables tailoring of the critical nanopost parameters to best suit the analysis of particular microorganisms and also to potentially separate and lyse the cells. Using LDI-MS on NAPA allows for multispecies analysis of metabolites without their isolation or the use of labels.[40] As a result, a more complete and rapid assessment of cellular responses to external and pathophysiological stresses, normal functional changes, or various mutations[41] can be observed in small ($1 < n \leq 100$) cell populations or using single cells.

The combination of direct cellular analysis on NAPA and metabolic network modeling on small populations will enhance our understanding of the roles of metabolic noise and provide needed insight into functional changes, as well as intracellular responses, to external and pathophysiological stresses. Further research is needed to broaden the coverage of the metabolome, including the metabolites involved in the biosynthesis of carbohydrates.

Received: September 12, 2012
Revised: December 19, 2012
Published online: February 27, 2013

Keywords: cellular differences · mass spectrometry · metabolites · nanostructures · single-cell analysis

[1] G. A. Evans, *Nat. Biotechnol.* **2000**, *18*, 127.
[2] H. B. Gutstein, J. S. MorriS, S. P. Annangudi, J. V. Sweedler, *Mass Spectrom. Rev.* **2008**, *27*, 316 – 330.
[3] J. R. S. Newman, S. Ghaemmaghami, J. Ihmels, D. K. Breslow, M. Noble, J. L. DeRisi, J. S. Weissman, *Nature* **2006**, *441*, 840 – 846.
[4] D. R. Bandura, V. I. Baranov, O. I. Ornatsky, A. Antonov, R. Kinach, X. D. Lou, S. Pavlov, S. Vorobiev, J. E. Dick, S. D. Tanner, *Anal. Chem.* **2009**, *81*, 6813 – 6822.
[5] S. C. Bendall, E. F. Simonds, P. Qiu, E. A. D. Amir, P. O. Krutzik, R. Finck, R. V. Bruggner, R. Melamed, A. Trejo, O. I. Ornatsky, R. S. Balderas, S. K. Plevritis, K. Sachs, D. Pe'er, S. D. Tanner, G. P. Nolan, *Science* **2011**, *332*, 687 – 696.
[6] C. V. Rao, D. M. Wolf, A. P. Arkin, *Nature* **2002**, *420*, 231 – 237.
[7] A. Amantonico, J. Y. Oh, J. Sobek, M. Heinemann, R. Zenobi, *Angew. Chem.* **2008**, *120*, 5462 – 5465; *Angew. Chem. Int. Ed.* **2008**, *47*, 5382 – 5385.
[8] T. R. Northen, O. Yanes, M. T. Northen, D. Marrinucci, W. Uritboonthai, J. Apon, S. L. Golledge, A. Nordstrom, G. Siuzdak, *Nature* **2007**, *449*, 1033 – 1036.
[9] S. S. Rubakhin, E. V. Romanova, P. Nemes, J. V. Sweedler, *Nat. Methods* **2011**, *8*, S20 – S29.
[10] C. E. Sims, N. L. Allbritton, *Lab Chip* **2007**, *7*, 423 – 440.
[11] J. L. Griffin, *Philos. Trans. R. Soc. London Ser. B* **2004**, *359*, 857 – 871.
[12] S. Moco, B. Schneider, J. Vervoort, *J. Proteome Res.* **2009**, *8*, 1694 – 1703.
[13] J. I. Castrillo, A. Hayes, S. Mohammed, S. J. Gaskell, S. G. Oliver, *Phytochemistry* **2003**, *62*, 929 – 937.
[14] J. Højer-Pedersen, J. Smedsgaard, J. Nielsen, *Metabolomics* **2008**, *4*, 393 – 405.
[15] L. J. Li, R. W. Garden, J. V. Sweedler, *Trends Biotechnol.* **2000**, *18*, 151 – 160.
[16] A. Amantonico, P. L. Urban, S. R. Fagerer, R. M. Balabin, R. Zenobi, *Anal. Chem.* **2010**, *82*, 7394 – 7400.
[17] B. Shrestha, A. Vertes, *Anal. Chem.* **2009**, *81*, 8265 – 8271.
[18] L. Wu, M. R. Mashego, J. C. van Dam, A. M. Proell, J. L. Vinke, C. Ras, W. A. van Winden, W. M. van Gulik, J. J. Heijnen, *Anal. Biochem.* **2005**, *336*, 164 – 171.
[19] Y. F. Shen, R. Zhang, R. J. Moore, J. Kim, T. O. Metz, K. K. Hixson, R. Zhao, E. A. Livesay, H. R. Udseth, R. D. Smith, *Anal. Chem.* **2005**, *77*, 3090 – 3100.
[20] S. G. Villas-Bôas, J. F. Moxley, M. Akesson, G. Stephanopoulos, J. Nielsen, *Biochem. J.* **2005**, *388*, 669 – 677.
[21] S. G. Villas-Bôas, J. Hojer-Pedersen, M. Akesson, J. Smedsgaard, J. Nielsen, *Yeast* **2005**, *22*, 1155 – 1169.
[22] J. Smedsgaard, J. Nielsen, *J. Exp. Bot.* **2005**, *56*, 273 – 286.
[23] K. F. Smart, R. B. M. Aggio, J. R. Van Houtte, S. G. Villas-Boas, *Nat. Protoc.* **2010**, *5*, 1709 – 1729.
[24] S. G. Ostrowski, C. T. Van Bell, N. Winograd, A. G. Ewing, *Science* **2004**, *305*, 71 – 73.
[25] M. E. Kurczy, P. D. Piehowski, C. T. Van Bell, M. L. Heien, N. Winograd, A. G. Ewing, *Proc. Natl. Acad. Sci. USA* **2010**, *107*, 2751 – 2756.
[26] G. Sun, K. Yang, Z. D. Zhao, S. P. Guan, X. L. Han, R. W. Gross, *Anal. Chem.* **2007**, *79*, 6629 – 6640.
[27] B. N. Walker, J. A. Stolee, D. L. Pickel, S. T. Retterer, A. Vertes, *J. Phys. Chem. C* **2010**, *114*, 4835 – 4840.
[28] B. N. Walker, T. Razunguzwa, M. Powell, R. Knochenmuss, A. Vertes, *Angew. Chem.* **2009**, *121*, 1697 – 1700; *Angew. Chem. Int. Ed.* **2009**, *48*, 1669 – 1672.
[29] J. A. Stolee, B. N. Walker, V. Zorba, R. E. Russo, A. Vertes, *Phys. Chem. Chem. Phys.* **2012**, *14*, 8453 – 8471.
[30] S. P. Gygi, B. Rist, S. A. Gerber, F. Turecek, M. H. Gelb, R. Aebersold, *Nat. Biotechnol.* **1999**, *17*, 994 – 999.
[31] J. Forster, I. Famili, P. Fu, B. O. Palsson, J. Nielsen, *Genome Res.* **2003**, *13*, 244 – 253.
[32] O. Fiehn, *Plant Mol. Biol.* **2002**, *48*, 155 – 171.
[33] B. N. Walker, J. A. Stolee, A. Vertes, *Anal. Chem.* **2012**, *84*, 7756 – 7762.
[34] A. Goffeau, B. G. Barrell, H. Bussey, R. W. Davis, B. Dujon, H. Feldmann, F. Galibert, J. D. Hoheisel, C. Jacq, M. Johnston, E. J. Louis, H. W. Mewes, Y. Murakami, P. Philippsen, H. Tettelin, S. G. Oliver, *Science* **1996**, *274*, 546 – 567.
[35] M. J. Herrgård, N. Swainston, P. Dobson, W. B. Dunn, K. Y. Arga, M. Arvas, N. Bluthgen, S. Borger, R. Costenoble, M. Heinemann, M. Hucka, N. Le Novere, P. Li, W. Liebermeister, M. L. Mo, A. P. Oliveira, D. Petranovic, S. Pettifer, E. Simeonidis, K. Smallbone, I. Spasic, D. Weichart, R. Brent, D. S. Broomhead, H. V. Westerhoff, B. Kirdar, M. Penttila, E. Klipp, B. O. Palsson, U. Sauer, S. G. Oliver, P. Mendes, J. Nielsen, D. B. Kell, *Nat. Biotechnol.* **2008**, *26*, 1155 – 1160.
[36] S. Wong, K. H. Wolfe, *Nat. Genet.* **2005**, *37*, 777 – 782.
[37] F. J. Bruggeman, N. Bluthgen, H. V. Westerhoff, *PLoS Comput. Biol.* **2009**, *5*, e1000506.
[38] G. Balázsi, A. van Oudenaarden, J. J. Collins, *Cell* **2011**, *144*, 910 – 925.
[39] M. G. Wiebe, E. Rintala, A. Tamminen, H. Simolin, L. Salusjarvi, M. Toivari, J. T. Kokkonen, J. Kiuru, R. A. Ketola, P. Jouhten, A. Huuskonen, H. Maaheimo, L. Ruohonen, M. Penttila, *FEMS Yeast Res.* **2008**, *8*, 140 – 154.
[40] M. R. Mashego, K. Rumbold, M. De Mey, E. Vandamme, W. Soetaert, J. J. Heijnen, *Biotechnol. Lett.* **2007**, *29*, 1 – 16.
[41] L. M. Raamsdonk, B. Teusink, D. Broadhurst, N. S. Zhang, A. Hayes, M. C. Walsh, J. A. Berden, K. M. Brindle, D. B. Kell, J. J. Rowland, H. V. Westerhoff, K. van Dam, S. G. Oliver, *Nat. Biotechnol.* **2001**, *19*, 45 – 50.

